ISSN 0036-0236, Russian Journal of Inorganic Chemistry, 2022, Vol. 67, No. 3, pp. 313–320. © Pleiades Publishing, Ltd., 2022.
Russian Text © The Author(s), 2022, published in Zhurnal Neorganicheskoi Khimii, 2022, Vol. 67, No. 3, pp. 334–341.

COORDINATION COMPOUNDS

Coordination and Spectral Properties of Oxa-Substituted Tetraphenylporphyrin Derivatives

S. G. Pukhovskaya[a], *, Yu. B. Ivanova[b], N. N. Kruk[c], A. O. Plotnikova[a], A. S. Vashurin[a], and S. A. Syrbu[b]

[a] *Ivanovo State University of Chemistry and Technology, Ivanovo, 153000 Russia*
[b] *Krestov Institute of Solution Chemistry, Russian Academy of Sciences, Ivanovo, 153045 Russia*
[c] *Belarusian State Technological University, Minsk, 220006 Belarus*
**e-mail: svetlana.puhovskaya@mail.ru*

Received September 8, 2021; revised September 18, 2021; accepted September 22, 2021

Abstract—Using theoretical conclusions from the Gouterman four-orbital model, a detailed analysis of the formation of absorption and fluorescence spectra of free bases and their zinc complexes has been performed for 5,10,15,20-tetraphenyl-21-oxaporphyrin and 5,10,15,20-tetraphenyl-21,22-dioxaporphyrin. The influence of the symmetry of the molecule on the position and shape of the bands in the electronic absorption and fluorescence spectra is shown. The kinetic parameters of the reactions of complexation of oxasubstituted derivatives of 5,10,15,20-tetraphenylporphine with *d*-metal salts (Cu(II), Zn(II), and Co(II)) at 288–308 K have been determined for the first time. The kinetic data obtained for oxasubstituted derivatives have been compared with results obtained for their classical analogue, tetraphenylporphine.

Keywords: porphyrins, metal complexes, electron-optical properties

DOI: 10.1134/S003602362203010X

INTRODUCTION

The structurally simplest porphyrin, porphine, is a tetrapyrrole macroheterocycle. In the reaction center of porphine there are four nitrogen atoms, which for the most part determine the properties of the molecule [1, 2]. Modification of the architecture of a molecule, as a rule, is carried out in two ways: first, by varying the nature and number of peripheral substituents, and secondly, by changing the macroring itself (hydrogenation, attachment of additional rings, and introduction of other heteroatoms). Substitution of pyrrole nitrogen by atoms of Group VIA leads to the formation of new macroheterocyclic systems, porphyrinoids or heterosubstituted porphyrins with unique little-studied properties that differ significantly from the properties of classical porphyrins [3]. The transformation of the reaction center inevitably affects the electronic structure of the macrocycle. At the same time, both physical and chemical properties of the compound change while maintaining the aromatic character of the π-electron system, stability, and the ability to form complexes with various metal cations. In recent years, the chemistry of heteroporphyrins has been developing rapidly: almost every analog of porphyrin and their derivatives, such as chlorins, corroles, tetrabenzoporphyrins, have been obtained, and the possibilities of their practical use as a more effective replacement for conventional metalloporphyrins have been determined [4].

The formation of complexes is an inalienable property of tetrapyrrole macrocycles; therefore, the study of the patterns of their preparation is an urgent and timely task of modern coordination chemistry.

It is known that tetrapyrrole macroheterocycles are effective converters of the primary analytical signal into the optical response of the sensor. They are characterized by fairly intense spectral-luminescent properties, in particular fluorescent ones, that can be used for these purposes. Tetrapyrrole molecules are intensively studied and, in some cases, are used as a source of an analytical signal, which contributes to solving problems associated with the detection and quantitative determination of the content of various ions in solutions. This area of chemistry has recently been actively developing with the aim of creating ion-sensitive materials [5].

This work presents the results of the study and analysis of the optical and coordination properties of 5,10,15,20-tetraphenyl-21-oxaporphyrin and 5,10,15,20-tetraphenyl-21,22-dioxaporphyrin, as well as their structural analog, 5,10,15,20-tetraphenylporphine.

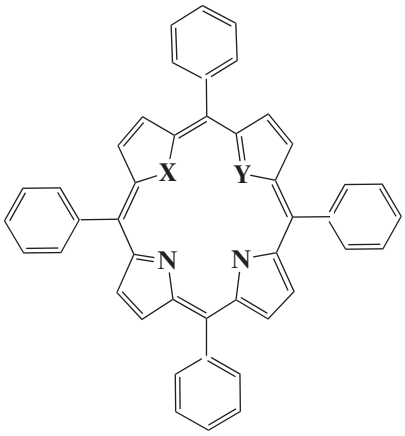

X = O, Y = N, HOTPP;
X = Y = O, O_2TPP;
X = Y = N, H_2TTPP.

EXPERIMENTAL

5,10,15,20-Tetraphenylporphine (H_2TPP, **I**), 5,10,15,20-tetraphenyl-21-oxaporphyrin (HOTPP, **II**), and 5,10,15,20-tetraphenyl-21,22-dioxaporphyrin (O_2TFP, **III**) were synthesized and isolated according to known methods. The spectral characteristics of the obtained compounds correspond to those reported [6–8].

5,10,15,20-Tetraphenylporphine (I). ESP (chloroform, λ (logε)): 413 (5.60), 513 (4.26), 546 (3.90), 590 (3.70), 650 (3.73). ^{1}H NMR (500 MHz, $CDCl_3$, δ, ppm): 8.30 (m, 8H, phenyl *o*-H), 7.80 (m, 12H, phenyl *m*- and *p*-H), 8.75 (8H, β-C), –3.75 (s, 2H, NH).

Anal. calcd. for $C_{44}H_{30}N_4$ (%): C, 86.11; H, 4.72; N, 9.16. Found (%): C, 86.12; H, 4.75; N, 9.12.

FAB: m/z = 613 (for $C_{44}H_{29}N_4$ anal. calcd. m/z = 613.24).

5,10,15,20-Tetraphenyl-21-oxaporphyrine (II). EAS (chloroform, λ (lgε)): 418 (5.41), 514 (4.36), 548 (3.81), 617 (3.48), 678 (3.69); ^{1}H NMR (500 MHz, $CDCl_3$, δ_H, ppm): 7.67 (m, *m*- and *p*-phenyl), 8.09 (t, *o*-phenyl), 8.46 (d, pyrrole), 8.52 (d, pyrrole), 8.80 (s, pyrrole), 9.10 (s, furan).

Anal. calcd. for $C_{44}H_{30}N_3O$ (%): C, 85.72; H, 4.88; N, 6.80; O, 2.58. Found (%): C, 85.71; H, 4.87; N, 6.81; O, 2.60.

FAB: m/z = 615 (for $C_{44}H_{29}N_3O$ anal. calcd. m/z = 615.73).

5,10,15,20-Tetraphenyl-21,22-dioxaporphyrine (III). EAS (DMF, λ (lgε)): 417 (4.93), 512 (3.91), 547 (3.72), 587 (3.53), 646 (3.41). ^{1}H NMR ($CDCl_3$, δ, ppm): 9.77 and 9.68 (d, 4H, furan); 9.01 and 8.94 (d, pyrrole); 8.16 (m, 8H, *o*-phenyl); 7.71–7.76 (m, 12H, *m*- and *p*-phenyl).

Anal. calcd. for $C_{44}H_{28}N_2O_2$ (%): C, 85.64; H, 4.55; N, 4.55; O, 5.29. Found (%): C, 85.55; H, 4.55; N, 4.65; O, 5.23.

FAB: m/z = 617.23 (for $C_{44}H_{28}N_2O_2$ anal. calcd. m/z = 616.71).

The synthesis and purification of zinc complexes with ligands (**I–III**) was carried out according to known methods [6, 9].

Solvents (acetic acid, DMF) and metal acetates pure for analysis (Russian State Standard) were purified by standard methods [10, 11].

Toluene (Aldrich, water content no more than 0.03%) used to measure fluorescence spectra was used without additional purification.

^{1}H NMR spectra of solutions of compounds **I–III** were recorded on a Bruker-500 spectrometer with an operating frequency of 500 MHz in $CDCl_3$. Tetramethylsilane was used as an internal standard.

The fluorescence spectra of tetrapyrrole compounds and their complexes were measured on a Varian Cary Eclipse fluorometer at a temperature of 298 K.

The EAS of porphyrin solutions and the rate of reactions of the formation of complexes of porphyrins **I–III** were determined on a Shimadzu UV-1800 and a Hitachi U-2000 spectrophotometers.

The rate of the complexation reaction was measured using thermostatically controlled cuvettes in the temperature range from 288 to 348 K. The temperature fluctuation did not exceed 0.1 K.

The first kinetic order of the reaction of the formation of metalloporphyrins was determined on the basis of the linear dependence $\log(c^0_{H_2P}/c_{H_2P})$–τ, where $c^0_{H_2P}$ and c_{H_2P} are the initial and current concentrations of porphyrin.

The concentration of solutions during the experiment was monitored by the change in optical density. The kinetic experiment was carried out with a ~50–100-fold excess of the salt solution concentration in comparison with the macroheterocycle solution, which made it possible to calculate the effective rate

Table 1. Electronic absorption spectra of free bases and zinc complexes of porphyrins **I**–**III** in toluene

Porphyrin	Wavelength, nm				
	B_{xy}	$Q_y(0.1)$	$Q_y(0.0)$	$Q_x(0.1)$	$Q_x(0.0)$
H_2TPP	419.0	514.0	547.5	593.5	650.5
HOTPP	420.5	507.5	541.5	614.0	674.0
O_2TPP	419.0	513.5	548.5	590.0	649.0
ZnTPP	423.0	–	–	549.0	589.0
ZnOTPP	428.0/444.5	548.0	591.0	583.0	636.0
ZnO_2TPP	423.0	–	–	549.5	589.0

constants (k_{eff}) of the complexation reaction according to the pseudo-first order equation:

$$k_{eff} = (1/\tau)\ln[(A_0 - A_\infty)/(A - A_\infty)], \quad (1)$$

where A_0, A, and A_∞ are the optical density of the porphyrin solution at the initial moment, at the moment of time τ, and at the end of the reaction, respectively. The optical density of solutions was measured for each porphyrin at two wavelengths corresponding to the absorption maxima of the ligand and complex. In this case, the root-mean-square error in determining k_{eff} did not exceed 3%.

The rate constants of the $(n + 1)$ order were calculated using the equation

$$k_{n+1} = k_{eff}/c^n_{M(OAc)_2}, \quad (2)$$

where n is the order of reaction (2) with respect to salt $M(OAc)_2$.

The activation energy (E_a) for the studied temperature range was calculated using the Arrhenius equation:

$$E_a = 19.1[(T_1T_2)/(T_2 - T_1)]\log(k_2/k_1), \quad (3)$$

where k_2 and k_1 are the effective rate constants of the reaction at T_2 and T_1, respectively, and the entropy of the transition state formation process ($\Delta S^{\neq}$) was calculated according to the equation:

$$\Delta S^{\neq} = 19.1\log k_v + E_a/T - 253. \quad (4)$$

RESULTS AND DISCUSSION

The replacement of one or two central nitrogen atoms with chalcogen atoms leads to significant changes in the electrical and optical properties of the obtained tetrapyrrole and macroheterocycles in comparison with their classical analogs (Table 1).

A detailed analysis of the formation of absorption spectra of free bases at 21- and 21,23-heterosubstitution reported [12] allowed us to conclude that there are significant changes in the configurational composition of electronic transitions.

As a result of these changes, the $Q_x(0.0)$ band of the long-wavelength electronic transition of 21-ONTPP in toluene, in comparison with the corresponding band of the H_2TPP molecule, is bathochromically shifted from 650 to 674 nm, and the maximum of the $Q_y(0.0)$ absorption band is hypsochromically shifted to 542 nm. The opposite direction of the spectral shifts of the absorption bands $Q_x(0.0)$ and $Q_y(0.0)$ is explained using the four-orbital Gouterman model [13] (Fig. 1 shows the distribution of the electron density on the molecular orbitals of the macrocycle).

When phenyl substituents are introduced into the C_m positions of the macrocycle, the energy of the b_1 orbital noticeably increases, and the one-electron configuration $b_1 \rightarrow c_1$ makes the greatest contribution to the configurational composition of the transition. Monooxa-substitution leads to a decrease in the energy of the b_1 and c_1 orbitals due to the lower electron density on the heteroatom, and an increase in the electron density on the C_a and C_b carbon atoms causes a slight increase in the energy of the b_2 and c_2 orbitals. Thus, the $Q_x(0.0)$ band of the long-wavelength electronic transition undergoes a bathochromic shift, while the $Q_y(0.0)$ band is hypsochromically shifted. A similar mechanism was proposed to explain the progressive bathochromic spectral shifts with an increase in the number of heteroatoms in the macrocycle in 21,23-heteroporphyrins [12].

Replacement of neighboring pyrrole rings with furan rings (21,22-substitution) leads to a slightly different character of the spectral shifts (Table 1). This is due to the fact that, first, the symmetry of the 21,22-substituted derivatives is lower than that of the 21,23-substituted derivatives, and, secondly, the different nature of the shifts of the molecular orbitals. Thus, the energies of the b_1 and c_1 orbitals decrease approximately in the same way, which leads to the fact that the energy of the dominant one-electron configuration $b_1 \rightarrow c_1$ practically does not change: the maximum of the $Q_x(0.0)$ absorption band is observed at 649 nm. The c_2 orbital tends to decrease in energy due to the lower electron density on the heteroatom, which is due to the combined action of negative inductive and

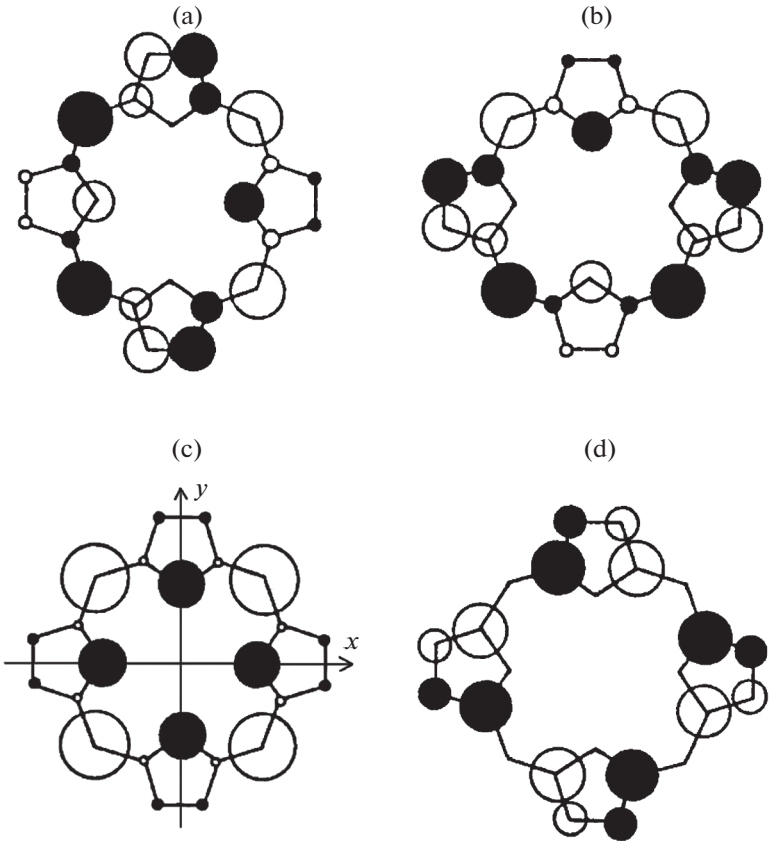

Fig. 1. LUMO and HOMO of the porphyrin macrocycle: (a) LUMO c_1; (b) LUMO c_2; (c) HOMO b_1; (d) HOMO b_2. The size of the circles is proportional to the atomic orbital coefficients. The positive and negative signs of the coefficients are shown with white and black circles, respectively. Axis x is directed along NH–NH (O–NH or O–O) and axis y is directed along N–N.

stronger mesomeric effects. However, at the same time, the c_2 orbital tends to increase its energy due to an increase in the electron density on the C_a and C_b carbon atoms. As a result, the position of the c_2 orbital practically does not change. A similar situation is observed for the b_2 orbital. As a result of the totality of these interactions, the electronic absorption spectrum of 21,22-O_2TPP practically does not differ from the absorption spectrum of the initial H_2TPP (Table 1).

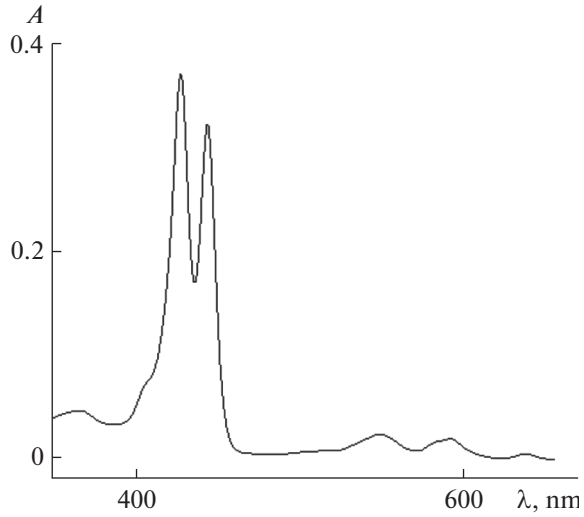

Fig. 2. Absorption spectrum of ZnONTPP in toluene.

The formation of metal complexes of 21- and 21,22-oxasubstituted TPP molecules with the Zn^{2+} ion is accompanied by significant changes in the electronic absorption spectra; however, they have a more complex structure than the spectra of metal complexes of "classical" porphyrins. Let us consider the formation of the electronic absorption spectrum of the ZnOHTPP molecule (Fig. 2).

The spectrum is characterized by two features: first, three Q-bands are observed in the visible region of the spectrum rather than two, as in "classical" metal complexes; second, the Soret band splits into two bands. The main reason for such spectral manifestations is, in our opinion, in the lower symmetry of the ZnOHTPP molecule in comparison with classical porphyrins. If the latter belong to the point symmetry group D_{4h}, then for metal complexes of 21-heteroporphyrins the symmetry cannot be higher than C_{2v}, as well as for their free bases, while the free bases of clas-

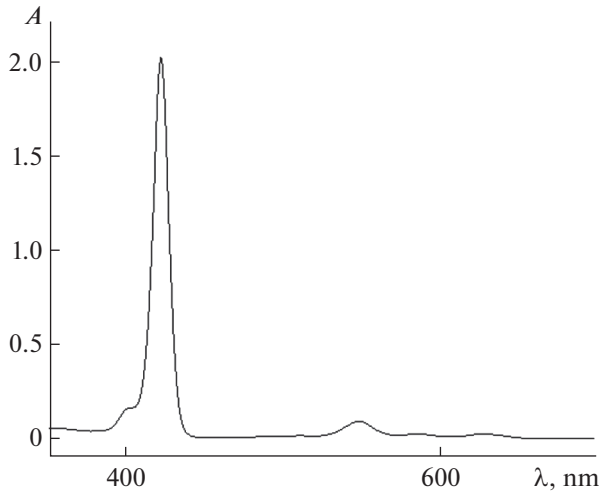

Fig. 3. Absorption spectrum of ZnO_2TPP in toluene.

sical porphyrins have the D_{2h} symmetry. The transition to a metal complex in classical porphyrins is accompanied by a twofold degeneracy of orbitals, the magnitude of the splitting between which at the free base of porphyrin is ~3000 cm^{-1} [14]. Due to the lower symmetry of the metal complexes of 21-heteroporphyrins, the molecular orbitals approach each other, but no degeneration is observed. As a result, the $Q_y(0.1)$ and $Q_y(0.0)$ satellite vibronic bandsof the first and second electronic transitions, respectively, are superimposed. Indeed, the second absorption band has an asymmetric profile with a maximum at 591 nm and a shoulder at 583 nm. If we take the shoulder at 583 nm as the $Q_y(0.1)$ band, and the maximum as the $Q_y(0.0)$ band, then for each of the electronic transitions the vibronic repetition frequency will be 1380 ± 50 cm^{-1}, and the splitting between electronic states is 1200 cm^{-1}, which is comparable to the splitting of the monoprotonated form of porphyrins belonging to the same point symmetry group [14]. Accordingly, due to the low symmetry, the Soret band splits into two components: B_x with a maximum at 444.5 nm and B_y with a maximum at 428 nm. Note that no splitting is observed for the 21-ONTPP free base, although the Soret band is noticeably broadened in comparison with the H_2TPP molecule. In our opinion, the differences are caused by the different degree of involvement of the heteroatom in the formation of the conjugated π-system. In the free base, the heteroatom is less "included," while in metal complexes the heteroatom is directly involved in the formation of the coordination bond with the metal ion and has a greater effect.

The symmetry of the ZnO_2TPP molecule increases (point symmetry group C_{2h}), as a result of which the Soret band is broadened, but not split into components, as in the ZnOHTPP molecule (Fig. 3). In the visible region of the spectrum, two absorption bands

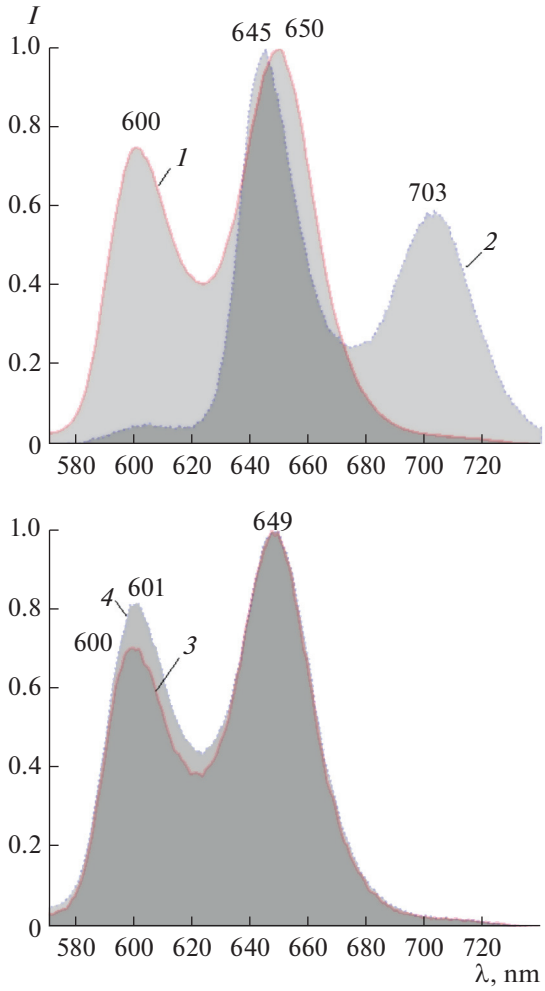

Fig. 4. Fluorescence spectra of zinc complexes normalized to the maximum: (*1*) ZnTPP, (*2*) ZnONTPP, (*3*) ZnTPP, (*4*) ZnO_2TPP. Excitation wavelength 500 nm.

are observed (Table 1), as in the case of "classical" porphyrins.

The investigated heteroporphyrins, both in the form of a free base and in the form of a metal complex, exhibit fluorescence. For fluorescence spectra, the frequency rule is satisfied, i.e. the position of the maxima in the fluorescence spectra is approximately mirror-symmetric to the position of the maxima in the absorption spectra (Fig. 4). The value of the Stokes shift for the ZnOHTPP molecule is 220 cm^{-1}, for the ZnO_2TPP molecule it increases to 340 cm^{-1}. An increase in the value when passing from the 21-oxa substituted derivative to the 21,22-dioxa-substituted derivative indicates an increase in relaxation processes in the lower excited singlet state. Indeed, according to X-ray diffraction data [15], the ZnOHTPP molecule has a nonplanar molecular macrocycle conformation. On the one hand, this is due to the fact that an axial ligand (salt counterion, acetate) is attached to the zinc ion, which induces the formation of a dome-shaped

Table 2. Kinetic parameters of the coordination reaction of 5,10,15,20-tetraphenyl-21-oxaporphyrin in comparison with 5,10,15,20-tetraphenylporphine with zinc, cobalt, and copper acetates in DMF*

Porphyrin	$C_{M(OAc)_2} \times 10^3$, mol/L	$k_{eff}^{298} \times 10^3$	k_v^{298}, L mol^{-1} s^{-1}	E_a, kJ/mol	$\Delta S^{\neq}$, J/(mol K)
			$Zn(OAc)_2$		
O_2TPP	1.3	No interaction			
HOTPP	1.3	8.97 ± 0.10	6.9 ± 0.02	57 ± 4	−45 ± 6
H_2TPP	1.3	6.52 ± 0.10	5.02 ± 0.02	61 ± 4	−35 ± 6
			$Co(OAc)_2$		
O_2TPP	1.5	No interaction			
HOTPP	1.5	2.25 ± 0.10	1.5 ± 0.02	62 ± 4	−100 ± 8
H_2TPP	1.7	0.15 ± 0.10	0.1 ± 0.02	91 ± 4	−46 ± 6
			$Cu(OAc)_2$		
O_2TPP	0.11	No interaction			
HOTPP	0.11	5.99 ± 0.02**	0.57 ± 0.02	8 ± 1	−232 ± 10
H_2TPP	0.11	0.02 ± 0.002**	0.002 ± 0.0002	20 ± 1	−200 ± 20

* The order of the reaction with respect to the salt in DMF was determined by the authors. [18]. **Dimension k_v^{298}, L$^{0.5}$ mol$^{-0.5}$ s^{-1}.

structure. On the other hand, a slightly smaller radius of the oxygen atom as compared to nitrogen causes the macrocycle to shrink and partially leave the plane of the furan ring with the formation of a corrugated macrocycle. The redistribution of the electron density in the excited state creates the prerequisites for structural relaxation, the value of which increases with an increase in the number of heteroatoms in the nucleus of the macrocycle.

The introduction of oxygen atoms into the macrocyclic ring leads not only to a change in the basicity of the compounds [16, 17] and the size of the inner cavity, but also to the absence of one or two protons in the nucleus. These changes significantly affect the characteristic properties of porphyrins such as aromaticity and metal binding capacity.

To date, the well-studied reaction of coordination of porphyrins by doubly charged transition metal cations in non-aqueous solvents occurs in accordance with Eq. (5), which has been convincingly shown in studies [1, 2]:

$$H_2P + [MX_2(Solv)_{n-2}] \rightarrow MP + 2HX + (n-2)Solv. \quad (5)$$

However, there are no data in the literature on the features of the course of coordination processes for heterosubstituted porphyrin analogs. In this work, the rate constants were measured for the first time and the energy parameters of the reaction of formation of zinc, copper, and cobalt complexes of heterosubstituted porphyrins **II** and **III** were determined in comparison with tetraphenylporphyrin in DMF (Table 2).

It is known that for classical porphyrins, reaction (5) obeys the kinetic equation of the first order with respect to the macrocycle [1, 2]:

$$-dc_{H_2P}/d\tau = kc_{H_2P}c_{MX_2}^n, \quad (6)$$

where k is the reaction rate constant, $c_{MX_2}^n$ is the salt concentration, and c_{H_2P} is the porphyrin concentration.

For all studied systems, we have found that the reaction of the formation of metalloporphyrins **II**, **III** also has the first kinetic order, which is confirmed by the straightforwardness of the dependences in the coordinates $\log(c_{H_2P}^0/c_{H_2P})-\tau$ ($c_{H_2P}^0$ and c_{H_2P} are the initial and current concentrations of the ligand) and the presence of clear isobestic points. Typical spectral changes during complexation are shown in Fig. 5.

As follows from the data listed in Table 2, we failed in measuring the kinetics of coordination of 5,10,15,20-tetraphenyl-21,22-dioxaporphyrin with acetates of the above metals in DMF; however, when acetic acid is used as a solvent, complexation is observed [17].

The replacement of one of the nitrogen atoms of the pyrrole fragment of the macrocyclic compound with an oxygen atom leads to an increase in the basic properties of the ligand by about two orders of magnitude [17]. The growth of a partial negative charge on the atoms of the reaction center promotes the strengthening of bonds with tertiary nitrogen atoms

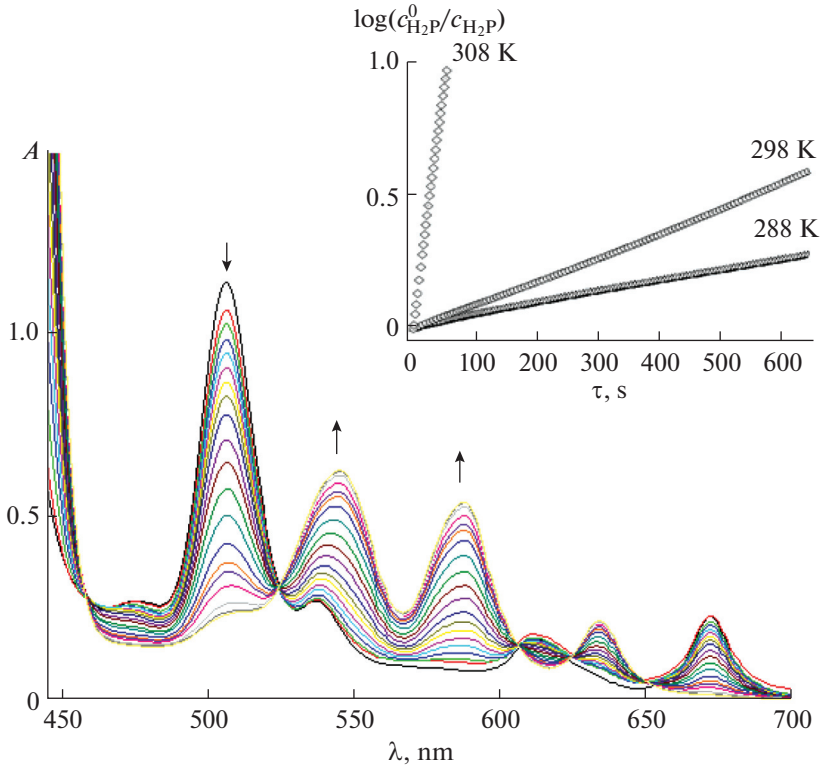

Fig. 5. Changes in electronic absorption spectra during the HOTPP coordination reaction with zinc acetate in DMF at 298 K. The inset shows the dependence $\log(c^0_{H_2P}/c_{H_2P})$ on τ for the reaction of ZnOTFP formation at 288, 298, and 308 K ($c_{Zn(OAC)_2}$ = 1.3×10^{-3} mol/L).

N → M in the transition state and thereby causes an increase in the rate of the complexation reaction in comparison with the classical analog. In the coordinating weakly basic solvent DMF, when passing from HOTFP to H_2TPP, the rate constant of the complexation reaction (5) increases with a simultaneous decrease in the activation energy. This is most clearly observed during the formation of copper complexes: the rate constant increases by ~280 times with a decrease in the activation energy by ~12 kJ/mol.

CONCLUSIONS

A detailed analysis of the formation of electronic absorption and fluorescence spectra of both free bases and zinc complexes of oxa-substituted tetraphenylporphine derivatives was carried out. It is shown that the position and intensity of the bands in the spectra are significantly influenced not only by the introduction of a heteroatom, but also by the geometry (symmetry) of the molecule. The mutually opposite influence of these factors leads to the spectra of 5,10,15,20-tetraphenyl-21,22-dioxaporphyrin, which is close to the classical H_2TPP; large differences are observed for 5,10,15,20-tetraphenyl-21-oxaporphyrin.

For the first time, the kinetics of coordination reactions of transition metal salts with oxasubstituted derivatives was studied in comparison with the classical analog of H_2TPP.

It was shown that the modification of the macrocycle by replacing one of the nitrogen atoms of the pyrrole fragment with an oxygen atom promotes an increase in the reaction rate with a regular decrease in the activation energy and entropy.

FUNDING

This work was carried out with the financial support of the Russian Foundation for Basic Research (grant no. 19-03-00214 A) using the equipment at the Collective Use Center "Upper Volga Regional Center for Physicochemical Research".

CONFLICT OF INTEREST

The authors declare that they have no conflicts of interest.

REFERENCES

1. B. D. Berezin, *Coordination Chemistry of Porphyrins and Phthalocyanine* (Nauka, Moscow, 1978) [in Russian].

2. B. D. Berezin and N. S. Enikolopyan, Metalloporphyrins (Nauka, Moscow, 1988) [in Russian].
3. S. A. Syrbu, S. G. Pukhovskaya, T. N. Dao, et al., Macroheterocycles **12**, 135 (2019). https://doi.org/10.6060/mhc190557s
4. P. Ziolkowski, J. Milach, K. Symonowicz, et al., Tumori. **81**, 364 (1995). https://doi.org/10.1177/030089169508100512
5. Kamaljit Singh, Amit Sharma, and Shivali Sharma, Adv. Heterocycl. Chem. **106**, 111 (2012). https://doi.org/10.1016/B978-0-12-396531-8.00002-X
6. Y. You, S. L. Gibson, R. Hilf, et al., J. Med. Chem. **46**, 3734 (2003). https://doi.org/10.1021/jm030136i
7. J. W. Buchler, *Synthesis and Properties of Metalloporphyrins. Porphyrins* (Academic Press, New York, 1978). https://doi.org/10.1016/B978-0-12-220101-1.50017-2
8. P. J. Chmielewski, L. Latos-Grażyński, M. M. Olmstead, et al., Chem. Eur. J. **3**, 268 (1997). https://doi.org/10.1002/chem.19970030216
9. Won-Seob Cho and Chang-Hee Lee, Bull. Korean Chem. Soc. **19**, 314 (1998).
10. Yu. V. Karyakin and I. I. Angelov, *Pure Chemicals* (Khimiya, Moscow, 1974) [in Russian].
11. A. Weissberger, Jr. and E. S. Proskauer, *Organic Solvents, Physical Properties and Methods of Purification* (Interscience Publishers, Inc., 1955).
12. I. V. Vershilovskaya, E. S. Lyul'kovich, S. G. Pukhovskaya, et al., Zh. Prikl. Spektr. **87**, 181 (2020).
13. M. Gouterman, *The Porphyrins*, vol. 3 (Academic Press, New York, 1978).
14. M. Kruk, A. Starukhin, and W. Maes, Macroheterocycles **4**, 69 (2011). https://doi.org/10.6060/mhc2011.2.01
15. R. Gloe, S. Suite, L. Goetzke, et al., Inorg. Chem. **52**, 1515 (2013). https://doi.org/10.1021/ic302268h
16. S. A. Syrbu, Y. B. Ivanova, S. G. Pukhovskaya, et al., Russ. J. Gen. Chem. **89**, 255 (2019). https://doi.org/10.1134/S0044460X19020148
17. S. G. Pukhovskaya, Y. B. Ivanova, A. O. Plotnikova, et al., Russ. J. Gen. Chem. **90**, 1292 (2020). https://doi.org/10.31857/S0044460X2007015X
18. E. M. Kuvshinova, S. G. Pukhovskaya, O. A. Golubchikov, et al., Koord. Khim. **19**, 630 (1993).

Translated by V. Avdeeva